Noninvasive diagnosis of seed viability using infrared thermography

Ilse Kranner[a,1], Gerald Kastberger[b], Manfred Hartbauer[b], and Hugh W. Pritchard[a]

[a]Seed Conservation Department, Royal Botanic Gardens, Kew, Wakehurst Place, West Sussex RH17 6TN, United Kingdom; and [b]Institute of Zoology, University of Graz, 8010 Graz, Austria

Edited by Maarten Koornneef, Wageningen Agricultural University, Wageningen, The Netherlands, and approved January 4, 2010 (received for review December 11, 2009)

Recent advances in the noninvasive analyses of plant metabolism include stress imaging techniques, mainly developed for vegetative tissues. We explored if infrared thermography can be used to predict whether a quiescent seed will germinate or die upon water uptake. Thermal profiles of viable, aged, and dead *Pisum sativum* seeds were recorded, and image analysis of 22,000 images per individual seed showed that infrared thermography can detect imbibition- and germination-associated biophysical and biochemical changes. These "thermal fingerprints" vary with viability in this species and in *Triticum aestivum* and *Brassica napus* seeds. Thermogenesis of the small individual *B. napus* seeds was at the limit of the technology. We developed a computer model of "virtual pea seeds," that uses Monte Carlo simulation, based on the heat production of major seed storage compounds to unravel physico-chemical processes of thermogenesis. The simulation suggests that the cooling that dominates the early thermal profiles results from the dissolution of low molecular-weight carbohydrates. Moreover, the kinetics of the production of such "cooling" compounds over the following 100 h is dependent on seed viability. We also developed a deterministic tool that predicts in the first 3 hours of water uptake, when seeds can be redried and stored again, whether or not a pea seed will germinate. We believe that the early separation of individual, ungerminated seeds (live, aged, or dead) before destructive germination assessment creates unique opportunities for integrative studies on cell death, differentiation, and development.

aging | crop | germination | imaging | stress

Seeds are attractive experimental model systems to study general biological phenomena, such as aging, cell death, and development. Desiccation tolerant "orthodox" seeds can be stored long term in the dry state, but lethal damage can be induced rapidly by "artificial aging," involving the elevation of seed moisture content (MC) and temperature (1). However, the biochemical and molecular interpretation of aging is hindered by the use of inseparable populations of viable and nonviable seeds, in which the partitioning of analytes in seeds of differential quality is unknown. Seed-quality studies would benefit from a tool that identifies individual viable and nonviable seeds before use. Moreover, global agriculture is fundamentally dependent on the production, distribution, and germination of high-quality seeds.

Pioneering studies (2–7) using microcalorimetry (8, 9) demonstrated that metabolic heat flows can be used to assess gross metabolism associated with germination processes. However, microcalorimeters do not capture thermal activity in the first phase of seed imbibition while samples equilibrate in the instrument. In addition, they are closed systems, preventing dissipation of heat and gas, with potential confounding feedback on seed metabolism. Consequently, these microcalorimetric studies were inconclusive as to whether temperature rises or falls during the initial stages of seed imbibition. These studies all focused on heat production by seeds, although some (3, 5) showed short phases of cooling, the significance of which was not appreciated. Hence, the mechanisms of heat production, and how they differ in viable and nonviable seeds, remained unclear. The aims of the present study were first, to investigate if infrared thermography (IRT), a fully noninvasive technique, can discern the thermal profiles of highly viable, aged, and dead seeds upon water uptake; second, to explore the biochemical basis of varying thermogenic activities in seeds of differential viability; and third, to develop an algorithm that predicts seed viability before germination. Garden pea (*Pisum sativum*) was used as the major model. Pea seeds do not display dormancy and lack of germination is clearly linked to viability loss. Wheat (*Triticum aestivum*) and rape seed (*Brassica napus*) were used to demonstrate the applicability of IRT to other seed types. Based on the findings presented, automated selection for seed viability could provide a tool for advancing studies of the molecular basis of seed aging and development.

Results

Artificial aging of *Pisum sativum* (L.) seeds produced differential viability (highly viable "A" to dead "E" populations), and seedlings with different root and shoot lengths (classified into "vigor types" 4 to 0; explanations in Fig. 1*A*). Highly viable seeds germinated when they reached a threshold MC of ~55%, found in untreated A and aged B seeds alike. Dead seeds took up water faster, but failed to reach this threshold MC (Fig. 1 *B* and *C*). Movie S1 (snapshots in Fig. 2*A*) shows changes in seed temperature of untreated and aged pea seeds, of which ~22,000 images per seed were analyzed every 20 s over 5 days to enable calculation of relative seed temperature (rT) (i.e., the difference between each individual seed and its immediate environment). Positive rT values reveal heat production; negative values denote cooling (i.e., negative heat production). In highly viable and vigorous A3&4 seeds, rT first showed a small peak (rT_{max}), then dropped sharply (rT_{drop}) within 1 h of imbibition, and reached a minimum (rT_{min}) shortly before radicle emergence (Fig. 2 *B* and *D*). While roots and shoots were produced, A3&4 seeds maintained rT at about −2 °C. In nonviable A0&1 seeds (i.e., a small proportion of seeds that were dead upon receipt), rT dropped earlier, then rose toward ambient temperature significantly faster (Fig. 2*B*).

Compared with untreated A seeds, artificially aged B seeds showed significantly delayed thermal profiles (Fig. 2*C*), associated with slower water uptake (Fig. 1*C*), indicative of changed membrane permeability. Seed MC and thermogenic activity of all seed types are shown in Figs. S1 and S2, demonstrating that t_{rTdrop} was gradually delayed with the length of aging treatment (compare A, B, and C seeds). By contrast, the mean temperature profiles of heat-killed E seeds showed the earliest t_{rTdrop} (Fig.

Author contributions: I.K., G.K., and H.W.P. designed research; I.K. and G.K. performed research; I.K., G.K., and M.H. contributed new reagents/analytic tools; M.H. developed a simulation model; I.K., G.K., and M.H. analyzed data; and I.K. and H.W.P. wrote the paper.

The authors declare no conflict of interest.

This article is a PNAS Direct Submission.

[1]To whom correspondence should be addressed. E-mail: i.kranner@kew.org.

This article contains supporting information online at www.pnas.org/cgi/content/full/0914197107/DCSupplemental.

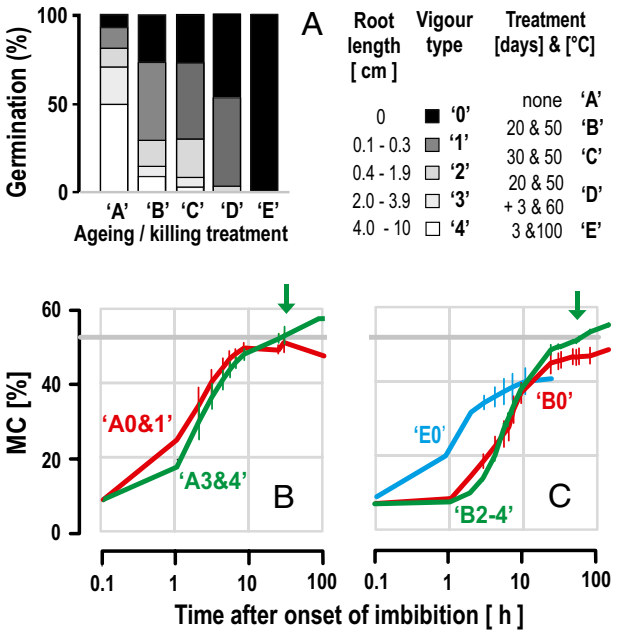

Fig. 1. Effects of aging on viability and MC of pea seeds. (*A*) Viability, defined as the percentage of germinated seeds, and vigor, classified by the root lengths of seedlings 5 days after sowing, following treatments A to E. Seeds were scored as germinated after radicle protrusion. The sum of vigor types 1 to 4 defines total germination. (*B*) Seeds that failed to germinate took up water faster but did not reach a threshold MC of 55% (gray horizontal line), here shown for nonaged A seeds (compare nonviable A0&1 seeds and viable A3&4) and (*C*) for aged B seeds (nonviable B0 versus viable B2–4 seeds) and heat-killed E seeds. Green arrows denote the time after which all viable seeds had germinated. MCs of all other seed types are shown in Fig. S1.

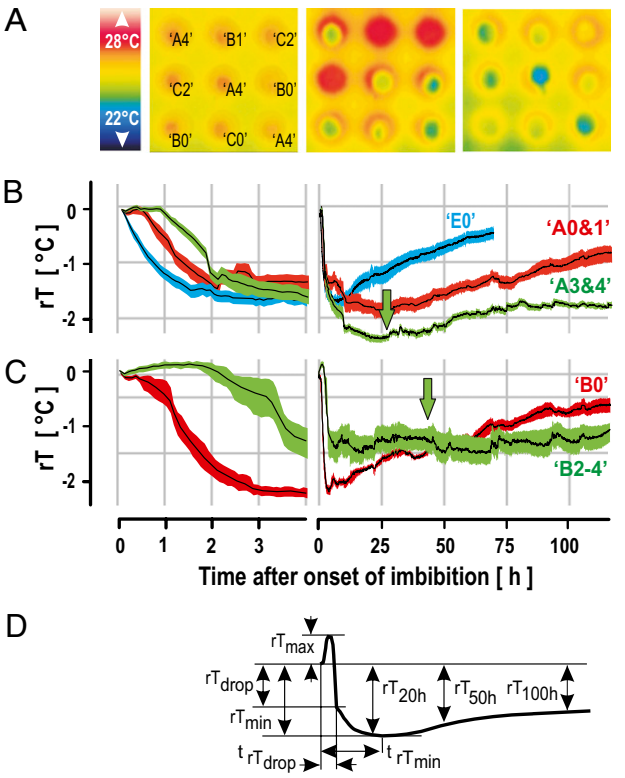

Fig. 2. Heat production during imbibition of pea seeds. (*A*) Snapshots from Movie S1. (*Left to Right*) Temperature scale and infrared thermographs of seeds 0, 4, and 80 h after onset of imbibition; note the radicle protrusion in the middle A seed in the last thermograph. (*B*) Early thermal profiles over the first 4 h (*Left*) and entire profiles (*Right*) over 5 days of untreated A seeds (green: viable, n = 73; red: dead, n = 18) and heat-killed E seeds (blue, n = 40) and (*C*) of aged B seeds (green: viable, n = 10; red: dead, n = 9). Black lines show mean values of data recorded with an infrared camera every 20 s and pooled in 5-min intervals, and the colored bands (i.e., merged vertical bars) show SE of means (statistical analyses in Table S1). Green arrows indicate completion of germination. Thermal profiles of all other seed types in Fig. S2 and correlation with MC in Table S2. (*D*) Schematic thermal profile of an individual seed with definition of characteristic parameters: drop, initial sharp drop in temperature; max, maximum; min, minimum; r, relative to ambient temperature; T, temperature; t, time.

2*B*), consistent with the highest rates of water uptake in the first hour of imbibition (Fig. 1*C*); thereafter, rT approached ambient temperature faster than in all other seeds.

Highly viable, fresh ("VF") wheat seeds also showed a small rT_{max} followed by a drop in temperature with a postgermination period of cooling, while rT in nonviable ("NV") seeds held at room temperature for 16 years rose toward ambient temperature (Fig. 3*A*), similar to rT in dead pea seeds. Viable, stored ("VS") wheat seeds held at 0 °C for 16 years were highly viable, but lost some vigor (they germinated later than VF seeds) and showed similar thermal profiles than VF seeds with less pronounced temperature fluctuations. Thermogenic activity was strongly correlated with seed mass (Fig. S3) and varied by two orders of magnitude between pea and rape seeds (Figs. 2 and 3). Thermogenesis in individual rape seeds was below the detection limit, but because of the abundance of data available over the entire time course, it was possible to show a trend of viable seeds maintaining negative rT, and of dead seeds equilibrating with ambient temperature (Fig. 3*B*). In summary, viable seeds of all three species showed significant variations in rT that were dominated by cooling. This cooling was produced by the seeds rather than evaporation. If evaporation was the cause, cooling would have been observed on the wet filter paper on which the seeds were germinated. Moreover, rT was calculated for each seed, so that the immediate environment of the seed (i.e., the filter paper) was subtracted from seed temperature.

We next explored the underlying mechanisms of seed thermogenesis using the pea model. We produced calibration curves for the thermogenic activities of principal seed storage compounds, visualizing the heat production of high molecular-weight (HMW) carbohydrates and the negative heat of solution of low molecular-weight (LMW) sugars (Movie S2; snapshots in Fig. 4*A*). We then generated a Java-based numeric simulation model using seed-specific concentrations and in vitro thermogenic activities of carbohydrates (Fig. 4*B*) upon imbibition to create virtual seeds (Fig. 5). The model simulates physico-chemical processes in seed thermogenesis on imbibition, and separates the contributions of cooling and warming components. Seed MC (Fig. S1) and previously published carbohydrate concentrations [data averaged from nine reports (10–18)] were used to approximate molar concentrations of carbohydrates in an imbibing real seed over time. Dry pea seeds contain 7.7% LMW sugars [0.4% monosaccharides (glucose and fructose), 2.7% sucrose, and 4.6% α-galactosides; that is, the "raffinose family"] and 43% starch that are immediately available for production of, respectively, negative and positive heat of solution upon water uptake. In the final stages of germination and thereafter, starch will be enzymatically degraded to maltose and glucose, again contributing to cooling. Pea seeds also contain highly concentrated noncarbohydrate storage compounds that produce positive heat of solution, namely proteins (25%) and cellulose (<5%), the heat production of which did not differ significantly from starch (per gram of compound), and in lower concentrations amino acids and salts, some of which produce negative heat of solution. The thermogenic activities of these compounds were not separately considered in the simulation model because an even greater number of variables would have compromised the depend-

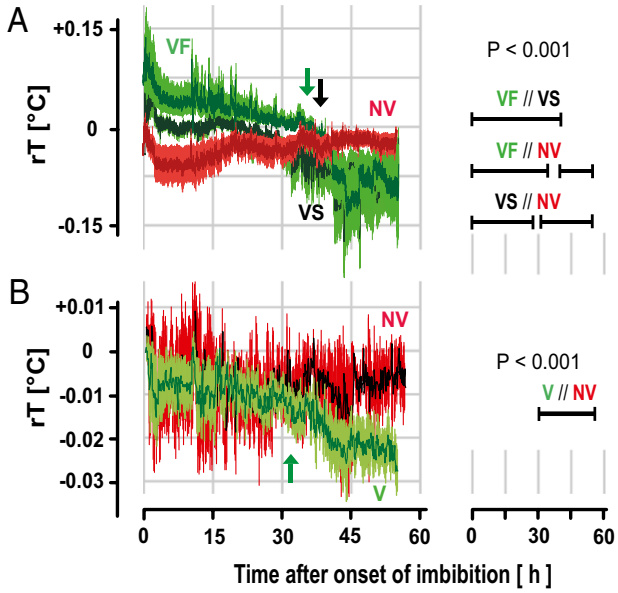

Fig. 3. Thermal profiles of wheat and rape seeds upon imbibition. (*A*) Wheat: the green line shows mean values of data recorded with an infrared camera every 20 s and pooled in 5-min intervals of highly viable, freshly harvested VF seeds and the vertical bars show SE of means (n = 80). Black line and green error bars denote viable seeds after 16 years of storage at 0 °C (VS, n = 72) and the dark red line and red error bars show means and SE of nonviable seeds after 16 years of storage at room temperature (NV, n = 80). (*B*) Rape seeds: The green line and vertical bars show means (recorded every 20 s and pooled in 20-min intervals) and SE of viable (V, n = 90) rape seeds after 14 years of storage at 0 °C and the black line with red error bars shows means and SE of NV (n = 110) seeds after 14 years in storage at room temperature. For rape seeds, measurements of single seeds were below the detection limit of the infrared camera and should not be overinterpreted, but it is worth noting that viable seeds still showed a clear drop at rT_{50h}, similar to viable wheat seeds. The bars on the far right of the graphs show time windows in which seed types differed significantly at $P < 0.001$.

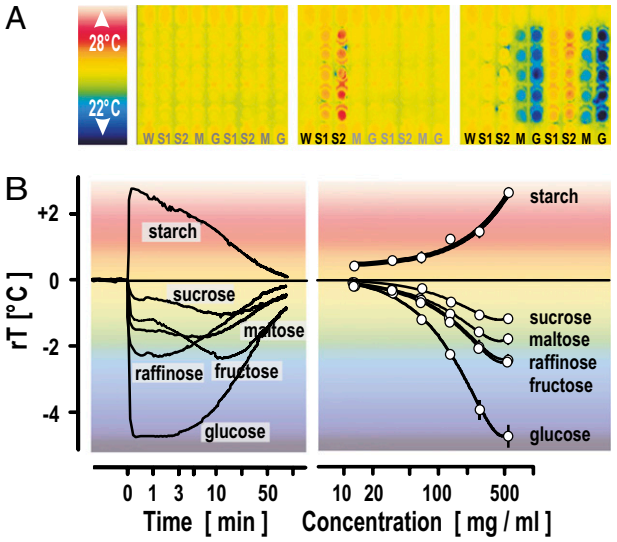

Fig. 4. Heat of solution of carbohydrates visualized by IRT, and quantified by image analysis. (*A*) Snapshots from Movie S2, showing positive heat of solution of starch, and negative heat of solution of maltose and glucose; color scale on the far left. In the infrared thermographs, each of five vials per column contained (*from Left to Right*): 800 μL water (W), 400 mg maize starch (S1), 400 mg soluble starch (amylose; S2), 400 mg maltose (M), or 400 mg glucose (G), and then again S1, S2, M, and G. (*Left*) Before experimentation, all chemicals and water were equilibrated at 24 °C; (*Middle*) After the addition of 800 μL water to the first vial, temperature increased rapidly in the starch-containing vials; snapshot taken after 1 min. (*Right*) Three minutes after addition of 800 μL water to the first vial the heat production in the first two columns S1 and S2 had already finished. Addition of water to glucose and maltose resulted in cooling. (*B*) Typical thermal profiles of HMW and LMW carbohydrates after the addition of water (0.5 g/mL; *Left*) and calibration curves (*Right*) obtained by plotting maximal (starch) and minimal (sugars) values of relative temperature against concentration; the background colors indicate the temperature scale; n = 5 ± SE; error bars within symbols have been removed.

ability of the simulation. Therefore, starch and the above-mentioned sugars were used, and should be viewed as representative of the entirety of thermogenically active molecules. The interactive internet model offers different options for the on-line simulation of the thermal profiles of virtual seeds at www.kfunigraz.ac.at/zoowww/erbthmod/Pea_model.html. Optionally, the simulation can disregard the contribution of starch (no heat production), the contribution of LMW sugars (no cooling), and the production of LMW sugars from starch degradation. Fig. 5 summarizes the model: without sugars, an imbibing virtual seed only dissipates heat, suggesting that negative heat of solution produced by sugars contributes to the thermal profile in a real seed. Without starch, rT would be too low to approximate real seed data. When the virtual seed is not allowed to produce LMW sugars from starch degradation at later stages of germination and after completion of germination, the simulated profile approximates the measured curve of nonviable seeds in which rT rose rapidly after rT_{min}, consistent with reduced activity of starch-degrading enzymes reported for aged seeds (e.g., wheat) (19).

We finally attempted to use the parameters defined in Fig. 2*D* for the prediction of seed viability in the first hours of germination when seeds can still be redried and restored; t_{rTdrop} and t_{rTmin} seemed particularly promising candidates, as they differed greatly within and between treatments (statistical details in Table S1). However, we were unsuccessful in using them, either on their own or in combination, to formulate a reliable algorithm that predicts the germinability of seeds with unknown viability. Therefore, we developed a deterministic tool that compares the entire time course over 4 hours of an unknown test seed with those of the mathematically modeled curves of the different seed types in A to E. The tool operates with iterative comparison of a thermal profile of an individual seed of unknown viability with the computed mean profiles of viable and nonviable seed types within and between treatments (modeled curves in Fig. S4 and equations in Table S3). Single viable A seeds can be distinguished from dead seeds with a success of up to 85% in less than 1 h (Fig. 6*A*) at which time the two seed types differ by $P < 0.001$. The tool can assess if an aged seed is alive or dead (Fig. 6*B*), if a viable seed was untreated or aged (Fig. 6*C*), and can separate heat-killed seeds from viable seeds with a success of up to 100% (Fig. 6*D*).

Discussion

Seed germination has been characterized by a triphasic curve of water uptake (20) (Fig. S5*A*). Membranes, mitochondria, and DNA are repaired and protein synthesis is reinitiated via stored mRNAs during Phases I and II (20, 21). Metabolism commences in Phase II with mitochondrial activity. Cell elongation at the end of Phase II and cell division in Phase III complete germination, and radicle protrusion is the visible result (20). As the seed approaches Phase III, it commits to forming a seedling and desiccation tolerance is lost; tolerance can only be regained through sophisticated manipulation within limited time windows (22). Pioneering research in the 1950s (2) and subsequent microcalorimetric studies recognized that pre- and postgermination heat flows vary with viability (3–7). Using microcalorimetry, viable and dead seeds could not be distinguished during sample equilibration in Phase I, which also hindered the appreciation of the significant cooling clearly revealed by IRT (Fig. 2). Importantly, early biochemical events in nondormant seeds in Phases I and II

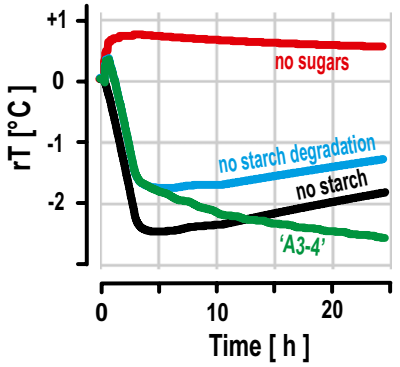

Fig. 5. Numeric model of pea seed thermogenesis, based on heat of solution of carbohydrates using seed MCs in Fig. S1 and calibration curves in Fig. 4*B*. rT, relative temperature. The green line shows a simulated curve for a viable nonaged (A3&4) seed; the red line shows a simulation in which no thermogenic activity of LMW sugars was permitted, demonstrating only positive heat of solution (no sugars); the black line shows a simulation without thermogenic activity of starch (no starch); and the blue line shows a simulation allowing only dissolution of starch and sugars present in the dry seed, but not degradation of starch into glucose at later stages of imbibition (no starch degradation). Further details can be found at www.kfunigraz.ac.at/zoowww/erbthmod/Pea_model.html.

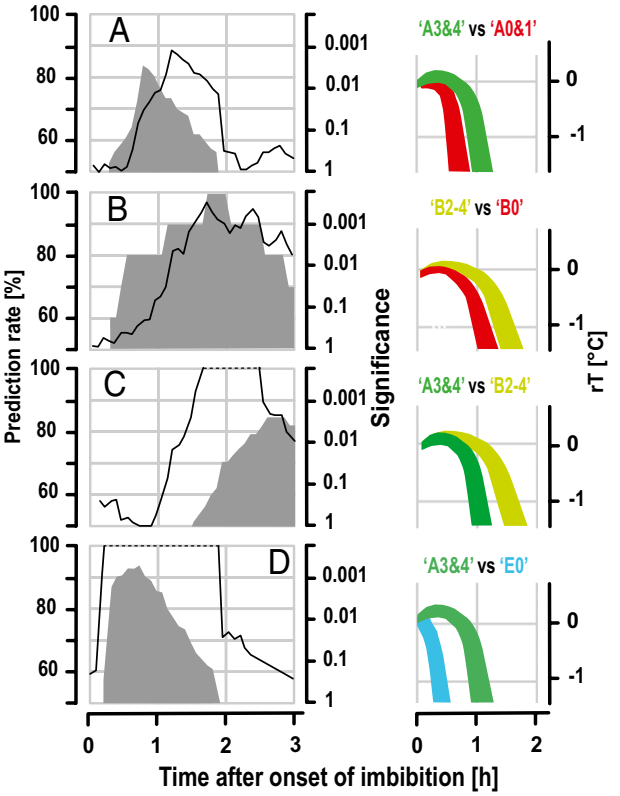

Fig. 6. Time windows in which pea seed viability can be predicted in the first 3 h of imbibition. rT, relative temperature; (*Left y* axes and gray time windows) Rate with which the viability of an unknown seed was successfully predicted. (*Middle y* axes and black lines) significance levels with which the mean values of two seed types differed over time. The schematics on the far right indicate the seed types tested. (*A*) Viable and dead seeds can be separated in untreated A seeds with a success rate of up to 85% after 50 min of imbibition. (*B*) Untreated A and aged B seed lots both produced viable seeds that differed in the third hour of imbibition. (*C*) Highly viable A seeds can be separated from heat-killed E seeds with a success rate of more than 90% after less than 30 min of imbibition and (*D*) highly viable A seeds can be separated from heat-killed E seeds, with a success rate of more than 90% after less than 30 min of imbibition.

are critical to whether a seed will germinate or die (23, 24). Nucleic acids, proteins, and lipids are inevitably subject to oxidative damage during seed maturation drying and, even more so, during storage and aging (25–28); repair very early in imbibition is key to successful germination (23–25).

There are three major contributions of this article. First, we show that IRT can diagnose the developmental stage of a germinating A pea seed, noninvasively and in real time. A small increase in rT to rT_{max}, followed by a sharp, pronounced rT_{drop} occurs in Phase I. A further, shallow decrease in rT follows until the end of Phase II, and rT_{min} coincides with the transition from Phase II to III, consistent with the onset of major reserves mobilization, such as starch breakdown into sugars (Fig. S5). In a germinating A3&4 seed, rT is relatively lower in Phase III than in a dead A0 seed (Fig. 2) that fails to produce cooling compounds, such as LMW carbohydrates from starch (Fig. 5). E seeds, killed by long-term heat treatment that resulted in enzyme denaturation (29), allowed us to address nonmetabolic, purely physico-chemical reactions. Compared to all other nonviable seeds, heat-killed E seeds were the first to reach rT_{drop}, related to the fastest initial water uptake, indicative of membrane degradation and massive cellular deterioration that follow heat-induced cytoplasmic glass melting (30). The marked rT_{drop} in all seeds, including those that are dead, strongly suggests that this initial temperature drop is nonmetabolic. After rT_{min}, rT rose rapidly toward ambient temperature in all nonviable seeds [being most pronounced in E (Fig. 2*B*)], strongly suggesting that the maintenance of low temperatures after rT_{min} in viable seeds in Phase II and thereafter is associated with cellular functionality. Thus, IRT produces a thermal fingerprint that clearly discerns seeds of differential viability and vigor.

The thermogenic activities of *T. aestivum* and *B. napus* seeds upon water uptake provide a proof of concept, confirming that IRT is applicable to other seed types. The three species used are taxonomically distant (monocotyledonous and dicotyledonous species in three different plant orders) and also represent different seed types regarding their reserve composition (starch and protein in pea, mainly starch in wheat, and mainly oil with only 4% starch in rape seed) and anatomy (details in Fig. S3 and ref. 31). The various methods used to induce seed death varied from natural (A pea seeds that were dead without any treatment), artificial aging (B to D pea seeds), heat-killing (E pea seeds), to long-term storage at room temperature (NV wheat and rape seeds). Nonetheless, the thermal profiles of live and dead seeds could be discerned across all aging treatments, species, and seed types.

Second, we attempted to link the noninvasively recorded thermal profiles of imbibing pea seeds to biochemical parameters that have been previously researched using invasive techniques (Fig. S5). Seeds will produce heat when water molecules lose kinetic energy as they bind to the helices of starch, and by metabolic processes such as the controlled uncoupling of respiration (32) that may involve uncoupling mitochondrial proteins related to the control of reactive oxygen species (33). As yet, cooling processes in imbibing seeds were addressed only once (34), but the significance and mechanisms of negative heat production were not understood. We explored the thermogenic activities of seed-storage compounds and used representative HMW and LMW compounds with thermogenic activity in a numeric simulation model to offer an explanation for the thermal signatures of imbibing seeds (Fig. 5). In orthodox seeds, maturation on the mother plant involves drying and accumulation of reserves and LMW sugars. These sugars contribute to the formation of a cytoplasmic glass essential for long-term survival in the dry state (35). Upon water uptake, they ensure rapid onset of vital functions in a germinating seed, and their dissolution cools the seed down. Our computer model can simulate heat flows upon seed imbibition and suggests that the thermal profiles in Phase I are dominated by

purely physico-chemical reactions, including the dissolution of LMW sugars in relation to the speed of water uptake; the maintenance of low temperatures at the end of Phase II and in particular in Phase III is linked to metabolism and reserve mobilization characteristic of viable seeds. Hence, IRT can link biochemical and biophysical parameters with developmental changes and visualize them noninvasively.

Third, IRT can also visualize in real time the earliest physico-chemical events in pea seed germination and diagnose seed viability in Phase I long before radicle emergence, after which seeds can still be redried and restored (36). Our deterministic tool (Fig. 6) allows prediction in the first 2 h of seed imbibition of whether an untreated A seed will germinate or die; it can also predict whether a viable seed was untreated (A) or aged (B or C) or killed by heat (E). IRT, in combination with this deterministic prediction tool, could be automated as a rapid, noninvasive, real-time seed viability test with considerable scientific benefits and potential economic value. Combined with reverse genetic approaches, IRT could enhance our knowledge of factors that determine seed germination, vigor, and viability. Seeds contain a whole organism in a small unit and are excellent experimental systems in which to study cell-aging, stress, and survival mechanisms that may have similar bases in plants, fungi, animals, and humans (26). Hence, the opportunity to select individual, live, aged, or dead seeds before experimentation opens previously unexplored avenues for studying mechanisms of cell aging and differentiation in individual organisms.

Methods

Seed Material and Statistics. Seeds of *Pisum sativum* L. cv Alaska Early were artificially aged (treatments A–E) at a constant MC of 10.0 ± 0.1%; details in *SI Methods* and Fig. 1. After two pilot experiments ($n = 2 \times 100$ seeds), three independent series of measurement were conducted ($n = 3 \times 100$ seeds; n for various seed types within treatments in Table S1). Germination tests were conducted separately on five replicates of 20 seeds per treatment. Another set of seeds was used in a detailed study of water uptake for which each individual seed was weighed at regular intervals (Fig. S1) ($n = 100$ for each treatment). Root lengths were recorded 5 days after sowing so that a temperature profile could be assigned to each individual seed. Temperature parameters, defined in Fig. 2*D*, were determined from each individual profile.

Seeds of *T. aestivum* L. var. *aestivum* and *B. napus* L. subsp. *napus* var. *napus* f. *biennis* (Schübl. and Mart.) were obtained from the Institute of Plant Genetics and Crop Plant Research (IPK). For each species, seeds of the same genotype were available that were either highly viable or had died during storage. Wheat seeds included VF seeds (highly viable, freshly harvested; total germination (TG) of > 98%), VS seeds (highly viable after storage at 0 °C for 16 years; TG > 95% TG), and NV seeds (nonviable after 16 years storage at room temperature). Two types of rape seeds used were V (highly viable after 14 years in storage at 0 °C; TG > 95%) and NV seeds (nonviable after 14 years in storage at room temperature; TG < 1%).

For all different seed types, means and SEs of thermal profiles were calculated. Data were tested for significance using one- or two-way ANOVAs in combination with least significant difference post hoc comparisons of means.

Infrared Thermography. A ThermaCAM SC3000 (Flir) with QWIP technology (advanced cooled long-wave Quantum Well Infrared Photodetector) and a sensitivity of 0.02 °C produced thermal images with a resolution of 320 × 240 pixels with high-speed data acquisition of 750 Hz PAL and real-time 14-bit digital output. Storage and analysis of infrared images are compatible with the ThermaCAM Researcher software (Flir). Sensor drifts in temperature were periodically reset by an internal shutter. The resulting temperature jitters were found in all pixels in an image and were corrected using references (e.g., the water bath), referred to as "camera-calibration reference temperature."

Care was taken to keep ambient temperature (both air and water) constant with minimal convection so that temperature gradients between seeds were minimal, and sufficient space between adjacent seeds was allowed so that the heat flows of individual seeds did not interfere. Conventional germination in Petri dishes on agar, sand, or filter paper proved unsuitable, because the lids prevented detection of seed temperature. Using infrared transparent foil instead of plastic or glass lids was unsuitable because of condensation of air humidity on the foil, resulting in little water droplets that produced erroneous images. When using Petri dishes without lids, the seeds initially imbibed and then dried slightly, failing to reach the critical MC required for germination. We therefore developed a germination method that uses polycarbonate plates (cryogenic vial holders 5030 from Nalgene) with 50 wells, each with an aperture at the bottom. When placed in a water bath (temperature kept constant at 24 °C, checked with an equilibrated thermometer), the plates floated and the wells were constantly filled with water. After covering the plates with filter paper, a little well-hydrated dip formed above each well in which one seed was placed, with the hilum facing downward as seeds with their hilum upward did not reach the critical MC required for germination (pea especially). Two 50-well plates were used for one series of measurement and were left undisturbed throughout the whole experiment.

Temperature data for each individual pea seed were calculated every 20 s over 5 d, and averaged at 5-min intervals. Digital sensors (5 × 5 pixels) were placed in the center of each seed image, covering approximately one-third of the seed area. The resulting temperature value, averaged over all pixels of the sensor area, is referred to as "seed temperature." A circular line sensor with the width of one pixel was arranged around the seed outside the zone affected by the thermogenic activity of the seed, providing the individual "seed calibration reference temperature". To correct for temperature gradients within the plates, rT was calculated as the difference between seed temperature and seed calibration reference temperature. For wheat, two sensors were used (5 × 5 pixels), one assessing $rT_{endosperm}$ the other rT_{embryo}. Data in Fig. 3 show $\Delta rT = rT_{endosperm} - rT_{embryo}$. Neither of these two rTs alone produced interpretable results, because the thermogenesis of individual wheat seeds was close to the detection limit of the infrared camera. The even smaller rape seeds also required additional referencing; for this, seeds were used that did not imbibe but were recorded simultaneously with the imbibing seeds.

Thermogenic activities of seed-storage compounds were tested by putting pure chemicals into plastic cuvettetes (maize starch, amylose, raffinose, sucrose, maltose, fructose, glucose, cellulose, and proteins). Water was added to each cuvettete, and temperature data recorded every 20 s (carbohydrate temperature) using area sensors (5 × 5 pixels). "Carbohydrate-calibration reference temperature" was determined by averaging values from 24 cuvettetes with water. rT in Fig. 4*B* denotes the difference between carbohydrate temperature and carbohydrate-calibration reference temperature; details in *SI Methods*.

Simulation of Seed Thermogenesis. A numeric, Java-based (Sun Inc.) computer model using NetLogo was developed that simulates pea thermal profiles using the known temperature kinetics of pure substances (starch, raffinose, sucrose, maltose, fructose, and glucose) dissolved in water (Fig. 4*B*); seed MC (Fig. S1) was used for the estimation of molar concentrations of these substances in seeds over time. Negative heat production was initially modeled using the thermal profile of raffinose and positive heat production was modeled using that of starch. Other different LMW sugars were added after the initial simulation steps were successful; details in *SI Methods*.

Deterministic Prediction Tool for Pea Seed Viability. Within a seed treatment (A–E), two categories were defined, nonviable and viable (e.g., A0&1 and A3&4) and polynomial fits of their temperature profiles calculated (Fig. S4 and Table S3). The rT values of the fitted curves were used as references for further testing. The thermal profile of an individual test pea seed was then compared with both references in the first 3 h of imbibition. The rT profiles of test peas were not included in the calculation of reference rT profiles. Results in Fig. 6 are based on 25-min test periods, in which predictions were made every 5 min. The decision (viable or nonviable) that was reached most often (at least three out of five) was taken as final within one test period. Consecutive test periods were started every 5 min and their final decisions recorded. Corresponding to 3 h of imbibition, 36 tests were conducted for a test pea. This procedure was repeated for all available test peas and the prediction rate is defined as the success of correct prediction; details in *SI Methods*.

ACKNOWLEDGMENTS. We thank Prof. H. Wilfried Pfeifhofer for invaluable discussions of the experimental design, Prof. Sir Peter R. Crane and Prof. J. Derek Bewley for support and critical comments on the manuscript, Reinhold Stachl and nbn Electronics, Graz, for loan of a Flir ThermaCAM sc 3000 and a ThermaCAM P620, and Dr. Andreas Börner, Institute of Plant Genetics and Crop Plant Research Gatersleben for providing *Triticum aestivum* and *Brassica napus* seeds. The Millennium Seed Bank Project is supported by the Millennium Commission, the Wellcome Trust, Orange Plc., and Defra. The Royal Botanic Gardens, Kew receive grant-in-aid from Defra.

1. Roberts EH (1973) Predicting the viability of seeds. *Seed Sci Technol* 1:499–514.
2. Prat H (1952) Microcalorimetric studies on germinations of cereals. *Can J Bot* 30:379–394.
3. Mourik J, Bakri A (1991) Application of microcalorimetry to plant technology: germination and initial growth. *Thermometric Application Note* 22017.
4. Hageseth GT, Cody AL (1993) Energy-level model for isothermal seed germination. *J Exp Bot* 44:119–125.
5. Sigstad EE, Prado FE (1999) A microcalorimetric study of *Chenopodium quinoa* Willd. seed germination. *Thermochim Acta* 326:159–164.
6. Edelstein M, Bradford KJ, Burger DW (2001) Metabolic heat and CO_2 production rates during germination of melon (*Cucumis melo* L.) seeds measured by microcalorimetry. *Seed Sci Res* 11:265–272.
7. Qiao YM, Wang RJ, Bai YG, Hansen LD (2005) Characterizing critical phases of germination in winterfat and malting barley with isothermal calorimetry. *Seed Sci Res* 15:229–238.
8. Criddle RS, et al. (1991) Simultaneous measurement of metabolic heat rate, CO_2 production, and O_2 consumption by microcalorimetry. *Anal Biochem* 194:413–417.
9. Wadso I (2000) Trends in isothermal microcalorimetry. *Thermochim Acta* 347:73–86.
10. Canibe N, Bach Knudsen KE (1997) Digestibility of dried and toasted peas in pigs. 1. Ileal and total tract digestibilities of carbohydrates. *Anim Feed Sci Technol* 64:293–310.
11. Knudsen KEB (1997) Carbohydrate and lignin contents of plant materials used in animal feeding. *Anim Feed Sci Technol* 67:319–338.
12. Abreu JF, Bruno-Soares AM (1998) Chemical composition, organic matter digestibility and gas production of nine legume grains. *Anim Feed Sci Technol* 70:49–57.
13. Gouveia A, Davies SJ (1998) Preliminary nutritional evaluation of pea seed meal (*Pisum sativum*) for juvenile European sea bass (*Dicentrarchus labrax*). *Aquaculture* 166:311–320.
14. Ereifej KI, Haddad SG (2000) Chemical composition of selected Jordanian cereals and legumes as compared with the FAO, Moroccan, East Asian and Latin American tables for use in the Middle East. *Trends Food Sci Technol* 11:374–378.
15. Kadlec P, et al. (2001) Processing of yellow pea by germination, microwave treatment and drying. *Innov Food Sci Emerg Technol* 2:133–137.
16. Urbano G, et al. (2005) Effects of germination on the composition and nutritive value of proteins in *Pisum sativum*, L. *Food Chem* 93:671–679.
17. Urbano G, et al. (2005) Nutritional assessment of raw and germinated pea (*Pisum sativum* L.) protein and carbohydrate by in vitro and in vivo techniques. *Nutrition* 21:230–239.
18. Costa GED, Queiroz-Monici KDS, Reis SMPM, de Oliveira AC (2006) Chemical composition, dietary fibre and resistant starch contents of raw and cooked pea, common bean, chickpea and lentil legumes. *Food Chem* 94:327–330.
19. Bernal-Lugo I, Rodriguez M, Gavilanes-Ruiz M, Hamabata A (1999) Reduced aleurone α-amylase production in aged wheat seeds is accompanied by lower levels of high-pl α-amylase transcripts and reduced response to gibberellic acid. *J Exp Bot* 50:311–317.
20. Bewley JD (1997) Seed germination and dormancy. *Plant Cell* 9:1055–1066.
21. Rajjou L, et al. (2004) The effect of alpha-amanitin on the Arabidopsis seed proteome highlights the distinct roles of stored and neosynthesized mRNAs during germination. *Plant Physiol* 134:1598–1613.
22. Buitink J, et al. (2006) Transcriptome profiling uncovers metabolic and regulatory processes occurring during the transition from desiccation-sensitive to desiccation-tolerant stages in *Medicago truncatula* seeds. *Plant J* 47:735–750.
23. Chen D, Osborne DJ (1970) Hormones in translational control of early germination in wheat embryos. *Nature* 226:1157–1160.
24. Osborne DJ, Dellaquila A, Elder RH (1984) DNA repair in plant cells - an essential event of early embryo germination in seeds. *Folia Biol (Prague)* 30:155–160.
25. Kranner I, Birtic S (2005) A modulating role for antioxidants in desiccation tolerance. *Integr Comp Biol* 45:734–740.
26. Kranner I, Birtic S, Anderson KM, Pritchard HW (2006) Glutathione half-cell reduction potential: A universal stress marker and modulator of programmed cell death? *Free Radic Biol Med* 40:2155–2165.
27. Bailly C, El-Maarouf-Bouteau H, Corbineau F (2008) From intracellular signaling networks to cell death: the dual role of reactive oxygen species in seed physiology. *C R Biol* 331:806–814.
28. Rajjou L, et al. (2008) Proteome-wide characterization of seed aging in Arabidopsis: A comparison between artificial and natural aging protocols. *Plant Physiol* 148:620–641.
29. Adams JB (1991) Review: Enzyme inactivation during heat processing of foodstuffs. *Int J Food Sci Technol* 26:1–20.
30. Bernal-Lugo I, Leopold A (1998) The dynamics of seed mortality. *J Exp Bot* 49: 1455–1461.
31. Finch-Savage WE, Leubner-Metzger G (2006) Seed dormancy and the control of germination. *New Phytol* 171:501–523.
32. Hourton-Cabassa U, et al. (2004) The plant uncoupling protein homologues: a new family of energy-dissipating proteins in plant mitochondria. *Plant Physiol Biochem* 42: 283–290.
33. Vercesi AE, et al. (2006) Plant uncoupling mitochondrial proteins. *Annu Rev Plant Biol* 57:383–404.
34. Baranowski P, Mazurek W, Walczak RT (2003) The use of thermography for pre-sowing evaluation of seed germination capacity. *Acta Hortic* 604:459–465.
35. Hoekstra FA (2005) Differential longevities in desiccated anhydrobiotic plant systems. *Integr Comp Biol* 45:725–733.
36. Harris D (2006) Development and testing of "on-farm" seed priming. *Adv Agron* 90: 129–178.